MICRO-DOPPLER EXTRACTION FROM ISAR IMAGE

Feng Li, Jun Cao, Lixiang Ren, Teng Long

Beijing Key Laboratory of Embedded Real-Time Information Processing Technology
School of Information and Electronics, Beijing Institute of Technology
Beijing, China

ABSTRACT

The micro-Doppler is an effective tool for target recognition. It is hard to detect micro-Doppler induced by vibration for its small value. In our system, phase-modulated stepped-frequency waveform is used. The method of matching pursuit (MP) is introduced to compensate translation. Translation trajectory is approximated by Chebyshev polynomial to improve approximation accuracy under low signal-to-noise ratio. The parameters in the polynomial are estimated by MP. To improve the performance of MP, simulated annealing is used. The operation of translation parameters estimation is performed in frequency domain before pulse compression. After translation compensation and pulse compression, Doppler component induced by rotation is mitigated by phase fitting. After compensation of translation and rotation, micro-Doppler is extracted from the result of motion compensation based on vibration model. Simulation and experiment data are used to testify our method.

Index Terms— Chebyshev polynomial, matching pursuit, micro-Doppler, simulated annealing, stepped-frequency waveform

1. INTRODUCTION

Different from traditional radar, synthetic aperture radar (SAR) can obtain azimuth resolution in the case of cooperative and stationary targets. Since azimuth resolution is obtained by processing Doppler phases of radar returns, it is also denoted as Doppler resolution. Different from SAR, Doppler resolution of inverse synthetic aperture radar (ISAR) [1] is the result of target's rotation by itself.

Micro-Doppler is an important characteristic of special targets. As [2] indicated, micro-Doppler is the result of target's micromotions. Micromotions of a plane can be classified as rotation and vibration. [3] and [4] focused on the discrimination of rotation parts from main body. Obviously the quality of ISAR imaging limits the extraction of rotation. Compared with rotation, vibration is relatively hard to be detected, since the amplitude of vibration is usually smaller than that of rotation. So smaller micro-Doppler is easily immersed in noise. [5] used fractional Fourier transform (FRFT) to detect vibrations in SAR. [6] used linear frequency modulation (FM) basis decomposition to estimate vibration frequency. [7] separated micro-Doppler from the body through time-frequency analysis. Micro-Doppler of vibration can also be estimated by the method of polynomial phase signal (PPS) [8]. Except heavy computation burden, PPS is not a maximum-likelihood estimation. Different from above methods, [9] directly fit the echo of micromotion based on vibration model [2]. In [9], orthogonal matching pursuit (OMP) [10] was used to treat the optimization problem to acquire vibration parameters. There are two difficulties in this method. First, OMP is used in discrete domain that limits the algorithm accuracy seriously. Second, the algorithm could not treat the Doppler decomposition resulted from rotation.

This paper introduces matching pursuit and simulated annealing to estimate translation parameters. Through phase extraction, rotation is compensated. Then vibration model is used to estimate the vibrating part in ISAR image. Section 2 describes the phase-modulated stepped-frequency signal. Micro-Doppler induced from vibration is expressed mathematically. Section 3 provides the method of translation compensation. In Section 4, we use phase-derived method to analyze micro-Doppler in ISAR image. Our method is testified through simulations and experimental data in Section 5 and 6 respectively. The conclusion is presented in Section 7.

2. SIGNAL MODEL

The geometrical model of ISAR imaging can be illustrated as Fig.1(a). In this model, radar is stationary. Target's motion can be classified into translation and rotation. Translation is in the direction of line-of-sight, which is used to describe the variation of the distance between range and target. In ISAR image, this dimension is called range or slant-range direction. Importantly, the translations of all scatterers are uniform. Target's rotation is the basis of cross-range resolution. The two dimensions are orthogonal. Through compression of received echo, range resolution is realized. Cross-range resolution is accomplished by

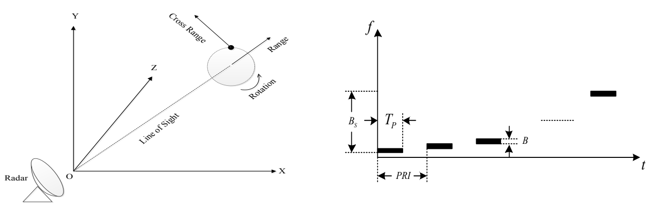

(a) (b)

Fig. 1. (a) Geometrical model of ISAR imaging. (b)Time-frequency distribution of transmitting bursts.

processing Doppler history of echoes at different times [1].

Stepped-frequency waveform [12] [13] is preferred for its narrow instantaneous bandwidth. High range resolution is achieved through synthesizing bandwidth. In [13], phase modulation is introduced into linear frequency modulation (LFM) waveform to improve the performance of ambiguity function. As LFM being replaced by constant carrier, a simplified version can be obtained and can be expressed as

$$u(t)=\frac{1}{\sqrt{T}}\sum_{k=1}^{K}\sum_{m=1}^{M}\exp\left[j\left(2\pi f_k t+\varphi_m\right)\right]\mathrm{rect}\left[\frac{t-(m-1)t_b-(k-1)t_p}{t_b}\right] \tag{1}$$

where t_b denotes the duration phase-modulated chip, t_p denotes pulse repetitive interval (PRI), f_k denotes stepped frequency, K is the number of scatterers, φ_m denotes modulated phase. The synthesized bandwidth is determined by the duration of phase-modulated chip and the number of stepped frequencies.

The time-frequency distribution of transmitting burst can be illustrated as Fig.1(b). In Fig.1(b), B denots bandwidth of phase-modulated pulse, T_p is the duration of pulse, B_s denotes synthesized bandwidth. Instantaneous bandwidth B is much smaller than synthesized bandwidth B_s.

Micro-Doppler is induced by micro-motions of a target or structures on targets. Micro-motions can be classified into rotation and vibration. Rotation part is easier to be detected [3] [4], since its micro-Doppler is larger and its SNR is higher. In many cases, vibrations' amplitudes are much smaller than theoretical resolution determined by transmitting bandwidth. So it is hard to be detected through pulse compression [16].

Without consideration of range migration and pulse compression, the phase of a scatterer's vibration induced by micro-Doppler can be expressed as [2]

$$s_R(t)=\sigma\exp\left\{j\frac{4\pi}{\lambda}R_0\right\}\exp\left\{j2\pi f_0 t+B_v\sin\left(\omega_v t+\theta_v\right)\right\} \tag{2}$$

In (2), vibration is determined by three parameters: B_v denotes vibration amplitude, ω_v denotes vibration frequency, and θ_v denotes initial phase. In (2), f_0 denotes Doppler frequency induced by the scatterer's rotation, which is determined by the distance between the scatterer and rotation axis. Moreover, λ is wavelength of carrier, R_0 denotes the scatterer's location in range, t is time variable in cross-range.

3. MOTION COMPENSATION

3.1 Translation Compensation Using Matching Pursuit

The motion compensation methods are based on range profiles. The range-compressed signal can be expressed as

$$ss(x,t)=\sum_{k=1}^{K}\sigma_k(x,y_k)\cdot\exp\left(-j4\pi\frac{x}{\lambda}\right)\cdot\Phi^T\left(R_o,v_T,a_T,t\right)\cdot\Phi^R\left(\omega_R,\alpha_R,x,y_k,t\right) \tag{3}$$

where

$$\Phi^T\left(R_o,v_T,a_T,t\right)=\exp\left\{-j\frac{4\pi}{\lambda}\left[\left(R_0+v_T t+\frac{1}{2}a_T t^2\right)+\cdots\right]\right\} \tag{4}$$

$$\Phi^R\left(\omega_R,\alpha_R,x,y_k,t\right)=\exp\left\{-j\frac{4\pi}{\lambda}\left[\omega_R y_k t+\frac{1}{2}\left(-\omega_R^2 x+\alpha_R y_k\right)t^2+\cdots\right]\right\} \tag{5}$$

In (3), σ is the scattering coefficient, subscript T denotes translation component, subscript R denotes rotation component. R_o, v_T, and a_T are parameters of translation. ω_R and α_R denote parameters of rotation. t is time variable in cross-range, λ is wavelength of carrier. x denotes range cell, and y_k is cross-range coordinate of scatterers. Since translation is identical to all scatterers, (3) could be rewritten as

$$ss(x,t)=\Phi^T\left(R_o,v_T,a_T,t\right)\cdot\sum_{k=1}^{K}\sigma_k(x,y_k)\cdot\exp\left(-j4\pi\frac{x}{\lambda}\right)\cdot\Phi^T\left(\omega_R,\alpha_R,x,y_k,t\right) \tag{6}$$

(6) could be viewed as being formed in target coordinate. In (6), the Φ^T could be compensated through range alignment.

Although the entropy method overcomes the problem of misalignment error accumulation, its performance is limited by the quality of profile image. The range profiles are the superposition of multiple scatterers, and they would vary with the angle of incidence. Thus for long coherent interval, the correlation between range profiles decreases. Then it is difficult to align the range profiles from the view of image. Because the optimization of range alignment is based on the image, the shift amounts moved by the algorithm are integer times of the sampling interval. This condition puts a boundary on the performance of range alignment. For non-LFM-type signal, such as phase-coded signal, the pulse compression without careful Doppler compensation, may lead to compression loss. Without Doppler compensation, the pulse compression of phase-coded would mismatch and the SNR of matching filter output would decrease.

In fact before pulse compression, it is feasible to obtain the motion parameter of the imaging target and to compensate the translate motion. Transforming echo into range frequency domain, it can be expressed as

$$Ss(\omega,t)=S(\omega)\cdot\sum_{k=1}^{K}\sigma_k\exp\left\{-j2\omega r_k(t)/c\right\}+n \tag{7}$$

(7) is formulated in transmitter coordinate. Different from (6), this expression is unique. In (7), ω denotes range frequency, t denotes cross-range time, $S(\omega)$ is spectrum of transmitting signal, σ_k is the scattering coefficient of the kth scatterer, c is the velocity of light, $r_k(t)$ is slant range of the kth scatterer at cross-range instant t, n is the measurement noise.

The parameters in (7) can be estimated by matching pursuit (MP) [11]. The method can avoid the negative effect of MTRC. Through constructing the basis function and calculating correlation with target echo, the parameters of the basis function can be estimated by optimization algorithm. In [9], orthogonal matching pursuit (OMP) is used to obtain optimum. Thus the suitable redundant dictionary should be carefully determined to reduce computation burden. In ISAR imaging, the amount of scatterers is limited. As the result, MP can estimate motion parameters of a single scatterer accurately.

3.2 Method of Chebyshev Polynomial

In many cases, the motion trajectory of the target could be generally approximated by polynomial. Intuitively, the higher order of the polynomial, the smaller is approximation error obtained. But a higher-order polynomial would result in heavy computational burden. Moreover, parameters estimation of target motion using higher-order polynomial might not converge. Taylor polynomial is a common tool for approximation. The concise form makes it able to be processed easily. It can be expressed as

$$r(t) = b_0 + b_1 t + b_2 t^2 + b_3 t^3 + \cdots \tag{8}$$

In (8), b_i is coefficients, t is time variable in cross range, $r(t)$ is range at the instant t.

However, different terms in Taylor polynomial are not orthogonal. Compared with orthogonal polynomial, Taylor polynomial needs higher order to obtain similar approximation accuracy. To acquire acceptable approximation accuracy in low order, we use Chebyshev polynomial [14] to describe translation. Chebyshev polynomial has orthogonal terms and can be expressed as

$$r(t) = a_0 U_0 + a_1 U_1 + a_2 U_2 + a_3 U_3 + \cdots \tag{9}$$

where

$$U_0 = 1,\ U_1 = t,\ U_2 = 2t^2 - 1,\ U_3 = 4t^3 - 3t \tag{10}$$

There are four types of Chebyshev polynomials [14], and they are equivalent in the issue of approximation.

4. MICRO-DOPPLER DERIVED FROM PHASE

4.1 Rotation Compensation

After translation compensation, the signal can be expressed as

$$s_R(t) = \sigma \exp\left\{ j \frac{4\pi}{\lambda} R_0 \right\} \exp\left\{ j2\pi f_0 t + B_v \sin(\omega_v t + \theta_v) \right\} \tag{11}$$

In (11), f_0 denotes Doppler, ω_v denotes vibration frequency, θ_v denotes phase, B_v is determined by the amplitude of vibration. From (11), the Doppler term induced by rotation is included. Simulation indicates that it is a hard to estimate vibration frequency (micro-Doppler) accurately without removing the Doppler. Therefore, Doppler should be compensated before micro-Doppler extraction.

From (11), compared with micro-Doppler, Doppler can be approached with lower-term series. Based on this principle, micro-Doppler component can be obtained through removal of low-order phase term from (11). This operation can be performed by phase fitting. After the Doppler is compensated, the result can be expressed as

$$s_v(t) = \sigma \exp\left\{ j \frac{4\pi}{\lambda} R_0 \right\} \exp\left\{ jB_v \sin(\omega_v t + \theta_v) \right\} \tag{12}$$

4.2 Micro-Doppler Extraction

The phase of vibration has the characteristic of cosine [17].

$$x(n) = \rho \exp\left\{ jA \cos(\omega n - \theta) \right\} \tag{13}$$

The micro-Doppler can be extracted by matching pursuit method. We can take (13) as basis function to perform MP. The maximum-likelihood estimation of vibration can be expressed as

$$(\omega, \theta) = \arg\max_{A,\omega,\theta} \mathrm{Re}\left\{ \frac{1}{N} \sum_{n=0}^{N-1} x(n) \exp\left[-jA\cos(\omega n - \theta) \right] \right\} \tag{14}$$

As an optimization problem, the cost function can be expressed as

$$\mathrm{Re}\left\{ \frac{1}{N} \sum_{n=0}^{N-1} x(n) \exp\left[-jA\cos(\omega n - \theta) \right] \right\} \tag{15}$$

It is a nonlinear optimization without constraint. Obviously, it can be resolved by gradient decent method. However, the main difficulty is to select step size. With a small step size, the resolution is accurate but the speed of convergence is slow. But with a large step size, residual error of the convergence is large. For a nonlinear optimization without constraints, iterative method [15] is a good candidate. This kind of method does not need to determine step size. But the obstacle of this algorithm appears when searching approaches optimum. When searching approaches an optimum, the convergence rate decreases significantly. Therefore, the speed of convergence slows down.

5. SIMULATION

5.1 Micro-Doppler Extracting of Vibrating Scatterers in Plane

5.1.1 ISAR Imaging of Plane without Vibration

Fig. 2(a) shows the structure of the simulated plane. Its ISAR Image result is given as Fig. 2(b). Because of no vibration added to the scatterers, defocusing in cross-range does not exist.

5.1.2 Vibrating Scatterer at the Wing of Plane

Vibration is added to the wing of the plane. As shown in Fig. 3(a), there is defocusing in cross-range at the wing of the plane. The vibration frequency is 10Hz. Moreover the range cell of the wing is analyzed by STFT and the time-frequency spectrogram is given as Fig.3(b), where the repetition frequency of the sinusoidal curve is 10 Hz.

Fig.4(a) and Fig. 4(c) show Taylor fitting and the micro-motion phase. Fig.4(b) and Fig.4(d) show Chebyshev fitting and relevant micro-motion phase. Sinusoidal curves are used to fit the micro-motion phases in Fig. 4(c) and (d). The frequency of micro-motion phase curve in Fig. 4(c) is 9.2 Hz, while that in Fig. 4(d) is 9.93 Hz.

6. EXPERIMENT

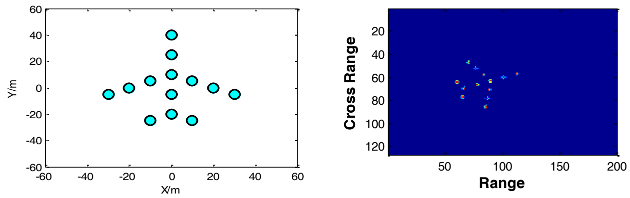

(a) (b)

Fig. 2. (a) Simulated plane. (b) ISAR image of simulated plane.

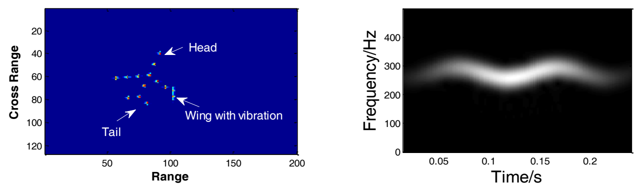

(a) (b)

Fig. 3. (a) ISAR imaging with vibrating scatter at the wing. (b) Time-frequency distribution of micro-Doppler.

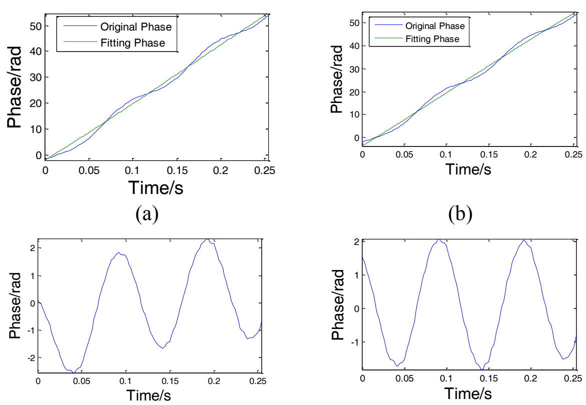

(a) (b) (c) (d)

Fig. 4. Extracting micro-Doppler of the plane wing. (a) Phase fitting of the wing's range cell with Taylor polynomial. (b) Phase fitting of the wing's range cell with Chebyshev polynomial. (c) Micro-motion phase by subtracting the Taylor fitting from the original phase; (d) Micro-motion phase by subtracting the Chebyshev fitting from the original phase. It performs more accurately than Taylor fitting.

The experimental system includes two antennas that are transmitter and receiver respectively as shown in Fig. 5(a). It is designed to image a plane. In experiment, the photo of imaged plane is shown as Fig. 5(b). The target plane is a Boeing 777 as shown in Fig. 5(c). The transmitter and receiver are placed on a platform that can be rotated. By rotating the platform by hand, we can keep the imaging target located in the mainlobe, since the motion of plane is slow relative to our radar platform.

The experimental parameters are listed as followings: center frequency 3 GHz, synthetic bandwidth 320 MHz, frequency step 5 MHz, subpulses number 64, subpulse width 0.1 us and pulse repetition interval 64 us. Take 128 bursts of returned signals for analysis. The ISAR image is shown as Fig. 6(a). Fit the phase of the range cell of the wing and the micro-motion phase is obtained as Fig. 6(b). The estimation of vibration frequency is 3.12 Hz.

7. CONCLUSION

This paper provides a method to extract the micro-Doppler induced by vibration. It is based on a series of range profiles. To analyze the Doppler phase of the same scatterer,

(a) (b) (c)

Fig. 5. (a) The photo of experimental system. (b) The photo of imaging target (Boeing 777) taken during the experiment. (c) The constriction of imaging target (Boeing 777).

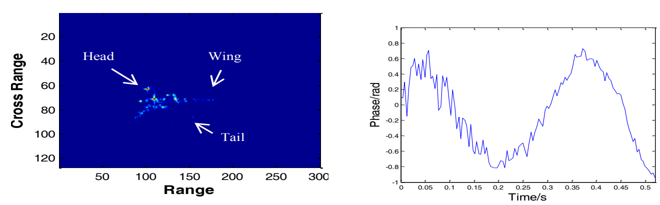

(a) (b)

Fig. 6. (a) ISAR imaging of 128 bursts. (b) The phase induced by vibration at the wing.

translation compensation is performed, which includes range alignment and phase correct. The phase induced by rotation is compensated to extract micro-Doppler. Based on vibration model, vibration frequency is estimated through correlation. In our method, both translation compensation and micro-Doppler estimation are based on correlation. Therefore they are also maximum-likelihood methods.

8. REFERENCES

[1] V. Chen. Time-Frequency Transforms for Radar Imaging and Signal Analysis. Boston, MA: Artech House, 2002.

[2] V. Chen, F. Li, S. Ho., and H. Wechsler, "Analysis of micro-Doppler signatures," *IEE Proc. Radar Sonar Navigat.*, vol. 150, no. 4, pp. 271-276, Aug. 2003.

[3] J. Li and H. Ling, "Application of adaptive chirplet representation for ISAR feature extraction from targets with rotating parts," *IEE Proc. Radar Sonar Navigat.*, vol. 150, no. 4, pp. 284-291, Aug. 2003.

[4] X. Bai, M. Xing, F. Zhou, G. Lu, and Z. Bao, "Imaging of micromotion targets with rotating parts based on empirical-mode decomposition," *IEEE Trans. Geosci. Remote Sens.*, vol. 46, no. 11, pp. 3514-3523, Nov. 2008.

[5] Q. Wang, M. Pepin, R. J. Beach, R. Dunkel, T. Atwood, B. Santhanam, W. Gerstle, A. W. Doerry, and M.M. Hayat, "SAR-based vibration estimation using the discrete fractional Fourier transform," *IEEE Trans. Geosci. Remote Sens.*, vol. 50, no. 10, pp. 4145-4156, Oct. 2012.

[6] P. Setlur, M. Amin, and F. Ahmad, "Analysis of micro-Doppler signals using linear FM basis decomposition," *SPIE* 2006.

[7] L. Stankovic, I. Djurovic, and T. Thayaparan, "Separation of target rigid body and micro-Doppler effects in ISAR imaging," *IEEE Trans. Aerosp. Electron. Syst.*, vol. 42, no. 4, pp. 1496-1506, Oct. 2006.

[8] S. Peleg and B. Porat, "Estimation and classification of polynomial-phase signals," *IEEE Trans. Inform. Theory*, vol. 37, no. 2, pp. 422-430, Mar. 1991.

[9] Y. Luo, Q. Zhang, C. Qiu, S. Li, and T. Yeo, "Micro-Doppler feature extraction for wideband imaging radar based on complex image orthogonal matching pursuit decomposition," *IET Radar Sonar Navig.*, vol. 7, no. 8, pp. 914-924, 2013.

[10] J. Tropp and A. Gilbert, "Signal recovery random measuremetns via orthogonal matching pursuit," *IEEE Trans. Inform. Thoery*, vol. 53, no. 12, pp. 4655-4666, Dec. 2007.

[11] S. Mallat and Z. Zhang, "Matching pursuits with time-frequency dictionaries," *IEEE Trans. Signal Process.*, vol. 41, no. 12, pp. 3397-3415, Dec. 1993.

[12] Y. Luo, Q. Zhang, C. Qiu, X. Liang, and K. Li, "Micro-Doppler effect analysis and feature extraction in ISAR imaging with stepped-frequency chirp signals," *IEEE Trans. Geosci. Remote Sens.*, vol. 48, no. 4, pp. 2087-2098, Apr. 2010.

[13] N. Levanon and E. Mozeson. *Radar Signals*. John Wiley & Sons, Hoboken, New Jersey, 2004.

[14] J. Mason, Chebyshev Polynomial: Theory and Applications. Norwell, MA: Kluwer, 1996.

[15] C. T. Kelley, *Iterative Methods for Optimization*. SIAM, Philaelphia, 1999.

[16] Y. Liu, D. Zhu, X. Li, and Z. Zhuang, "Micromotion characteristic acquisition based on wideband radar phase," *IEEE Trans. Geosci. Remote Sens.*, vol. 52, no. 6, pp. 3650-3657, June 2014.

[17] P. Setlur, M. Amin, and F. Ahmad, "Analysis of micro-Doppler signals using linear FM basis decomposition," *SPIE* 2006.